Adaptive optics system to accurately measure highly aberrated wavefronts

M. Ares and S.Royo

Center for Sensor, Instrumentation and System Development, Technical University of Catalunya
(www.cd6.upc.edu)
Rambla Sant Nebridi 10, E08222 Terrassa Spain

ABSTRACT

Due to the improvements in design and manufacturing technologies, new lenses with complex shapes are continuously appearing in the market. The fabrication of free-form lenses depends mainly on the possibility of measurement. A sensor with simultaneously a large dynamic range and good resolution becomes essential to be able to produce complex-shaped lenses with high quality. Regarding this purpose, we propose an adaptive optics (AO) system to measure with a good resolution lenses that have a complex shape. The AO system consists in a novel Shack-Hartmann wavefront sensor based on a cylindrical microlens array, and a liquid crystal programmable phase modulator (PPM) as an active device within an open-loop configuration. The original wavefront from the lens to test is compensated with the PPM in order to decrease its complexity. Subsequently, the compensated wavefront can be measured by the sensor with good accuracy. The wavefront generation performance of the PPM was analyzed in order to evaluate its suitability for open-loop compensation, and a very good correlation between the theoretical wavefront written on the PPM and the measured wavefronts has been obtained for the different amounts of aberration studied. To validate the working principle of the complete setup, an spherical ophthalmic lens with a strong curvature that exceeds the dynamic range of the sensor was successfully measured.

 Keywords: Adaptive optics, Wavefront sensor, Shack-Hartmann, Dynamic range expansion, Liquid crystal phase modulator, Open-loop.

1. INTRODUCTION

The adaptive optics (AO) principle is based on the local modification of the phase of a distorted wavefront to compensate for its aberrations. Astronomy has traditionally been the main field of AO development, where compensation of atmospheric induced light distortions has allowed the ground based recording of high resolution

images[1]. Besides astronomical applications, in the past few years the AO technology has been incorporated into a variety of other optical areas. In the human vision field, the AO compensation of the eye's aberrations produces aberration free retinal images which may enhance the human vision. Moreover, a deeper knowledge of physical properties of a living retina has become possible by means of obtaining high resolution images of the retina "in vivo"[2]. The correction of laser wavefront distortions in external or internal cavities, or custom modifications of the original laser beam shape have also been successfully achieved by use of AO techniques[3,4].

Although AO systems can be rather complex, the basic principle is quite simple. In conventional AO, the distorted wavefront is measured with a wavefront sensor and compensated by introducing its conjugate in the phase correcting device by means of a control system. As mentioned, two optical elements are involved in every AO system to perform the wavefront compensation: a wavefront sensor and a phase correcting device. Different types of wavefront sensors are used depending on the application, such as interferometric sensors, Shack-Hartmann wavefront sensors (which combine a high speed of measurement and a large dynamic range), or curvature wavefront sensors (which have the advantage of simplifying the control procedure). The most usual active correcting devices are micromachined deformable mirrors (MMDM) and liquid crystal phase modulators. MMDMs are well-known devices, assembled in major large telescopes around the world, which have a very fast response for a real-time compensation. On the other side, liquid crystal phase modulators have a lower speed, but are able to compensate larger aberrations with a higher spatial resolution in a single step (open-loop) due to their more linear response.

2. ADAPTIVE OPTICS SYSTEM

Fig. 1 shows the AO system that we have constructed to measure highly aberrated wavefronts. A 635 nm point light source obtained from a laser diode coupled with a monomode optical fibre is collimated using a diffraction limited achromat. The resulting plane wavefront passes through a linear polarizer and crosses the object of interest (an ophthalmic lens in our case). The transmitted wavefront is directed towards the liquid crystal phase modulator (PPM) by means of a pellicle beam-splitter (BS) which does not change the optical path length. The aberrated wavefront is compensated and reflected by the PPM, which is conjugated with the cylindrical Shack-Hartmann sensor (CSHWS)[5] through a 4:1 telescope system. The microcylindrical array samples the wavefront under test creating a focal line pattern recorded by a ½" high resolution monochrome CCD detector. The array is placed onto a high-precision mechanical rotary stage, which allows the vertical and horizontal line patterns to be recorded, and, thus, the x and y directional wavefront slopes can be obtained. Subsequently, from these data, the wavefront is easily reconstructed in terms of the circular Zernike polynomial basis.
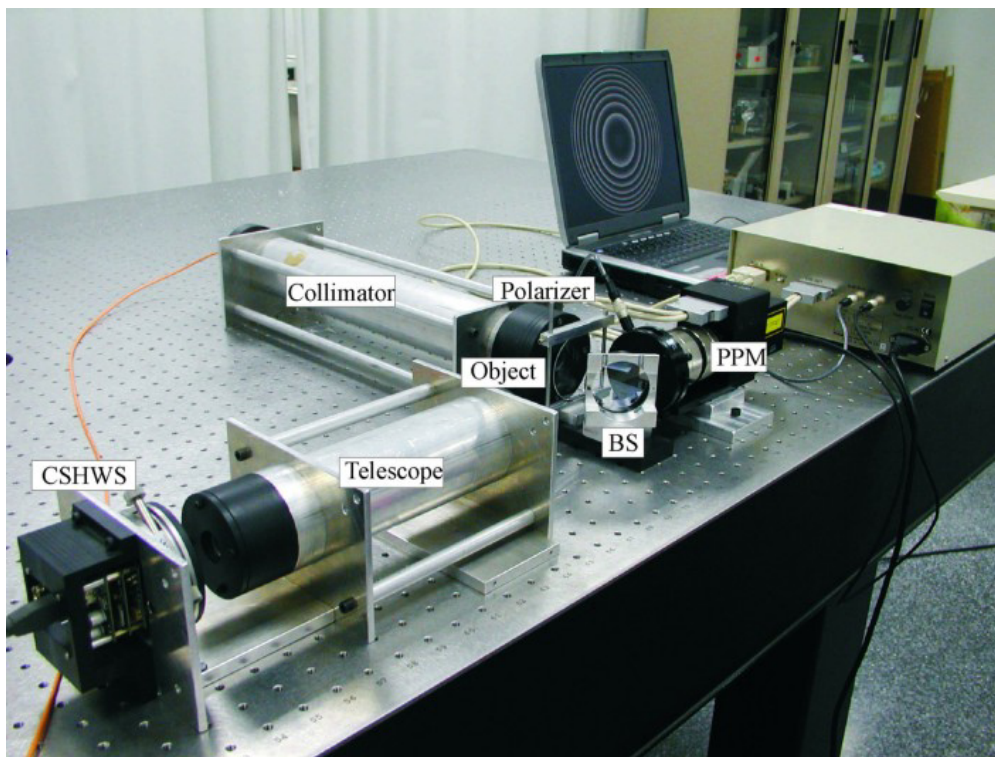
Fig. 1. AO system constructed to test commercial ophthalmic lenses with large departures from a plane shape.

2.1. Wavefront sensor

A novel Shack-Hartmann wavefront sensor based on a cylindrical microlens array (CSHWS) has been developed in order to extend the dynamic range of the classical Shack-Hartmann sensor (SHWS) with a good resolution of measurement ($\lambda/25$ at λ=635 nm used). The microcylinders focus the wavefront to be measured onto the CCD in the form of focal lines instead of the classical focal spots in the Shack-Hartmann sensor. This implies that the wavefront samples along a given focal line are continuously connected, allowing to perform a correct localization of all the data, even where the wavefront has steep curvatures or abrupt shape changes. The expansion of dynamic range using the CSHWS is illustrated in Fig. 2. As it may be seen, the part of the wavefront which is less aberrated and passes through the central column of the array of spherical microlenses (numbered as 1) or through the central microcylinder (1), is properly localized in both cases. However, in the wavefront area where steep phase changes appear, it may be noticed how in the conventional SHWS the spots tagged with capital letters leave their corresponding subapertures in area 3 and merge with those belonging to area 5. This implies an uncertainty in the assignment of spots a5 and A5, b5 and B?, and g5 and G5. As a consequence, there is a relevant loss of data for wavefront reconstruction purposes. The use of the CSHWS solves this problem as all the wavefront samples refracted by each microcylinder are connected in the same

focal line and may be easily tracked with simple algorithms. Thus, samples within lines number 5 and number 3 are unequivocally assigned to microcylinders 5 and 3, respectively.

Despite the abovementioned expansion, the CSHWS has a limited dynamic range due to the superposition of the lines of the pattern where a very highly distorted wavefront is involved. To overcome the CSHWS limit, the compensation provided by the phase modulator device within the complete AO system allows the successful measurement of higher distorted wavefronts.

(a)   (b)
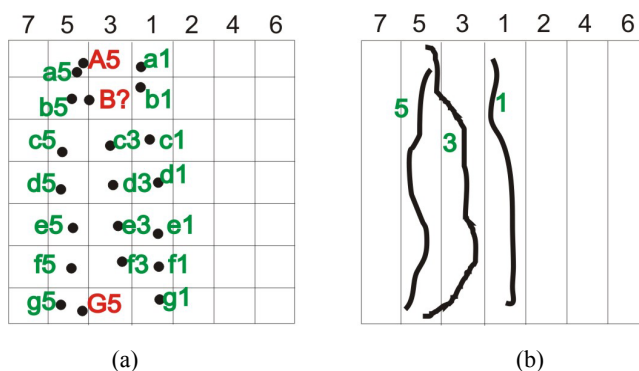
Fig. 2. Detected patterns of a complex wavefront with: (a) a conventional SHWS with spherical microlenses which has an uncertainty on the localization of some spots; and (b) the CSHWS from which all the data are correctly localized.

2.2. PPM operation

The PPM consists of an electrically-addressed intensity light modulator (LCD), optically coupled to a parallel-aligned liquid crystal spatial light modulator (PAL-SLM). In essence, the wavefront that we want to generate is computationally written on a 768 x 768 pixelated LCD as a wrapped grey level phase map. This intensity distribution is then imaged through a subsystem of microlenses into the PAL-SLM to lose the pixelated LCD structure and therefore to avoid the unwanted diffraction effects introduced by the pixel regular structure. Inside the PAL-SLM, the intensity distribution written on the LCD is transformed into a voltage distribution across the PAL by means of a α-Si:H photoconductive layer. On the application of the voltage distribution the originally parallel-aligned molecules tilt, the effective refractive index reduces, and, as a result, the phase of light in a given area locally advances[6]. The wavefront which interacts with the PAL-SLM is so compensated by this spatial phase modulation, although the effect only takes place if the wavefront is linearly polarized in parallel to the PAL-SLM molecules in their original relaxed state.

The PPM may be seen as a dynamic computer generated hologram with, therefore, the flexibility of match the exact conjugated wavefront shape of interest. Due to the performance with a wrapped phase representation (phase modulo λ), quite steep aberrated wavefronts can be produced. Nevertheless, unwanted diffractive effects appear as the amount of aberration increases. The diffraction efficiency (defined as the ratio of the intensity of the first order of diffraction related to the 0th order) decreases from 90% to less than 40% as the amount of aberration increases[7,8]. Thus, the first

order of diffraction, which contains the phase modulation, may be notably weak when compared to the 0th order light, which corresponds to the original wavefront reflected on the PAL-SLM surface. This spurious 0th order light must be disregarded when highly distorted wavefronts are used for compensation.

3. EXPERIMENTAL RESULTS

3.1. Wavefront generation performance of the PPM

To validate the compensation capabilities in open-loop, the wavefront generation performance of the PPM has been analyzed in terms of the amount of aberration considered. Following specifications of the manufacturer, the PAL-SLM was driven by a 3V square signal at 800 Hz in order to achieve a linear response of phase modulation of 2.5π at the wavelength used (635 nm). Spherical wavefronts of different curvatures (measured in diopters, as an inverse of the radius of curvature) were introduced in the 768 x 768 pixelated LCD of the PPM in wrapped phase map representation over the whole 20 x 20 mm liquid crystal active area. The incident plane wave in the PPM was modified and reflected as an output beam which should take the spherical shape introduced, and it was measured by the CSHWS. Fig. 3 shows, from left to right, the theoretical spherical wavefront that is written on the PPM, the intersected line patterns detected by the sensor, and the final reconstruction of the wavefront for the different amounts of aberration considered (0.25 D, 0.5 D, 1 D and 1.5 D). The line pattern images clearly show the diffractive behavior of the PPM device. The original plane wave interacts with the PPM and, as a result, it is split in several orders of diffraction with different intensities (basically the 0th and first orders). When creating a large aberration, the period of the wrapped optical path function which is written on the PPM is shortened, so the diffraction efficiency noticeably decreases; i.e. the intensity of the first order of diffraction (which is phase-modulated) becomes highly reduced with regard to the 0th order (which is the non-modulated original wavefront). As far as only the modified phase light is of our interest, the superimposed 0th order information is not taken into account when processing the image to reconstruct the wavefront. Table 1 shows the comparison between the theoretical wavefront written on the PPM and the measured wavefront for a 20 mm pupil. A relative RMS error below the 0.15% has been obtained in all cases, showing the excellent wavefront generation performance of the PPM and, therefore, its suitability for adaptive compensation in open-loop.
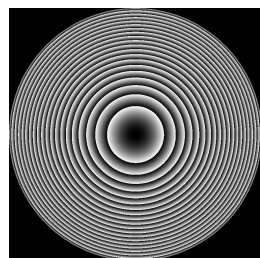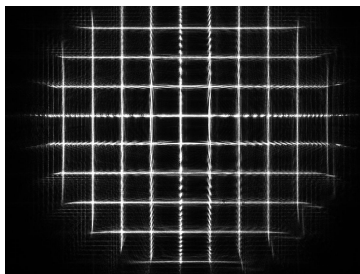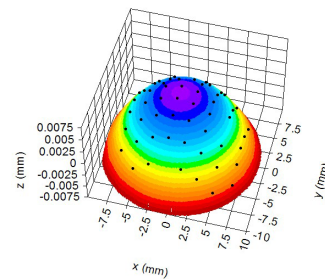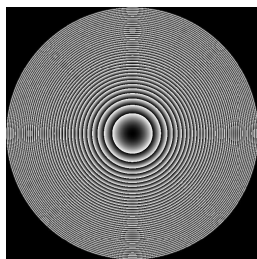
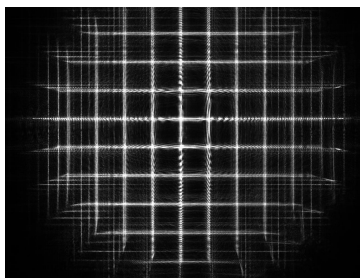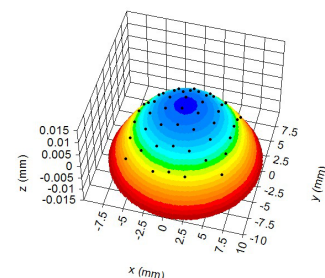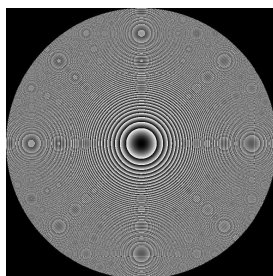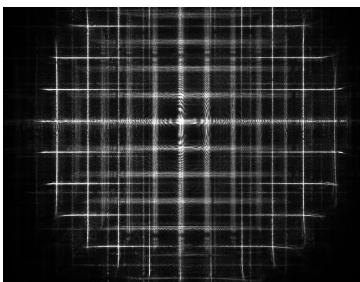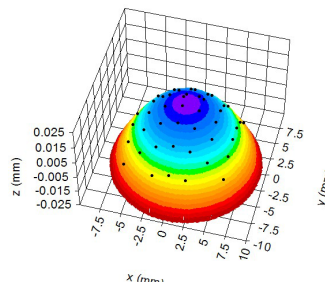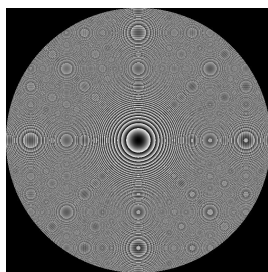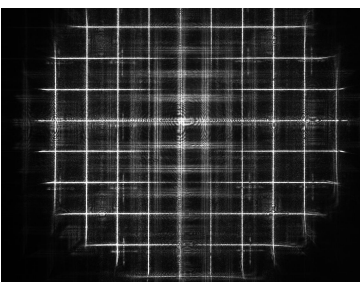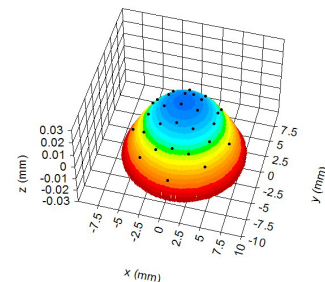Fig. 3. Wavefront generation results of the PPM where theoretical spherical wavefronts of 0.25 D, 0.5 D, 1 D and 1.5 D are created (a, d, g and j), measured with the CSHWS (b, e, h and k) and reconstructed (c, f, i and l).

Ideal Spherical Wavefront [diopters]	Ideal Spherical Wavefront PV [waves]	Measured Spherical Wavefront [diopters]	RMS difference [waves]
0.25	19.68	0.252	0.022
0.5	39.36	0.499	0.013
1	78.72	0.986	0.062
1.5	118.08	1.513	0.080

Table 1. Comparison between the ideal and measured spherical wavefronts

3.2. Compensation of a spherical wavefront

To validate the technique of measurement with the AO system, we measured the wavefront leaving a commercial spherical ophthalmic lens with a nominal spherical power of 2.75 D. A central circular area of 20 mm in diameter was scanned in a single shot, and the transmitted wavefront was initially tried to measure using the CSHWS. The intersection of the vertical and horizontal line patterns detected by the CSHWS without active compensation from the PPM is shown in Fig. 4a. As it may be observed, all focal lines become superimposed in the central region due to the strong curvature of the wavefront, which exceeds the dynamic range of the sensor. In this case, the localization of the lines is not possible and, as a consequence, the wavefront can not be measured. To overcome the measurement impossibility, an adaptive solution was carried out with the described setup. A divergent spherical wavefront with a power of -1.58 D (which is close to the limit of PPM generation) was written on the PPM. The wavefront transmitted by the spherical lens is propagated along the setup until it reaches the PPM as a 3.58 D spherical wavefront. The PPM then compensates the 3.58 D wavefront with the -1.58 D phase change written on it and, subsequently, transforms the previously non-measurable wavefront into a wavefront of 2.0D whose curvature may be measured by the CSHWS in a single shot. The intersection of the vertical and horizontal line patterns detected after the compensation is shown in Fig. 4b. As explained in Sec. 3.1, the spurious 0th-order diffractive artifact is superimposed to the first diffractive order containing the significant data. It should be noticed how the uncompensated line pattern in fig.4a is reproduced in the central region of Fig.4b, while the compensated wavefront data appears only in fig.4b. This makes more complex and time-consuming the image processing task, where the 0th-order data must not be considered. Even so, as opposed to the non-compensated situation, it was possible to properly measure the wavefront after an adaptive open-loop compensation, as shown in Fig. 4c. The measured wavefront has 2.0D, and has a P-V value of 157.47λ, while the initial spherical wavefront of 3.58D had a 281.98λ value.
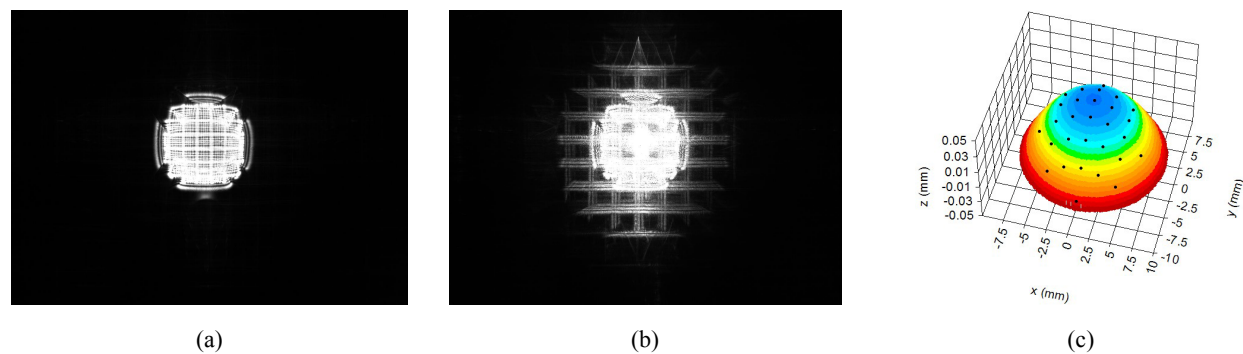
(a)　　　　　　　　　　　(b)　　　　　　　　　　　(c)

Fig. 4. Line patterns detected (a) before and (b) after the AO compensation from which the large curved spherical wavefront was measured (c).

4. CONCLUSIONS

We have presented an AO system developed to measure new commercial complex-shaped lenses. The AO system consists in a novel Shack-Hartmann wavefront sensor based on a cylindrical microlens array (CSHWS), and a liquid crystal programmable phase modulator (PPM) as an active device within an open-loop configuration. In order to know the suitability of the PPM in open-loop compensation, we have evaluated its wavefront generation performance for different amounts of aberration induced. We have compared theoretical spherical wavefronts of 0.25 D, 0.5 D, 1 D and 1.5 D written in the PPM with the real wavefronts measured, obtaining negligible differences for all the cases. The aberration compensation process was thus found to be linear, with the only drawback of a decrease of the diffraction efficiency for larger aberration amounts, which makes more difficult and time-consuming the image processing procedure in those cases. The diffraction problems might be reduced with a higher resolution device or by introducing a filter element to eliminate the 0th order light, a solution which is nowadays being developed. To validate the adaptive compensation technique, a spherical ophthalmic lens with a curvature which exceeds the dynamic range of the CSHWS was successfully measured with the whole AO system by partially compensating the converging wavefront with a diverging wavefront written on the PPM. The setup is equally valid for the compensation of large wavefront aberrations of complex shape.

ACKNOWLEDGEMENTS

REFERENCES

1. R.K. Tyson, "Principles of Adaptive Optics", 2ºEd., Academic Press, 1997.

2. P.M. Prieto, E.J. Fernandez, S. Manzanera and P. Artal, "Adaptive optics with a programmable phase modulator: applications in the human eye", Opt. Express, 12 (17), pp.4059-4071, 2004.

3. J.C. Chanteloup, H. Baldis, A. Migus, G. Mourou, B. Loiseaux and J.-P Huignard, "Nearly diffraction-limited laser focal spot obtained by use of an optically addressed light valve in an adaptive-optics loop", Opt. Lett., 23 (6), pp.475-477, 1998.

4. N. Sanner, N. Huot, E. Audouard, C. Larat, J.-P. Huignard and B. Loiseaux, "Programmable focal spot shaping of amplified femtosecond laser pulses", Opt. Lett., 30 (12), pp.1479-1481, 2005.

5. M. Ares, S. Royo and J. Caum, "Shack–Hartmann sensor based on a cylindrical microlens array", Opt. Lett., 32 (7), pp.769-771, 2007.

6. N. Mukohzaka, N. Yoshida, H. Toyoda, Y. Kobayashi and T. Hara, "Diffraction efficiency analysis of a parallel-aligned nematic-liquid-crystal spatial light modulator", Appl. Opt., 33 (14), pp.2804-2811, 1994.

7. Y. Igasaki, F. Li, N. Yoshida, H. Toyoda, T. Inoue, N. Mukohzaka, Y. Kobayashi and T. Hara, "High efficiency electrically-addressable phase-only spatial light modulator", Opt. Rev., 6 (4), pp.339-344, 1999.

8. M. T. Gruneisen, R. C. Dymale, J. R. Rotge, L. F. DeSandre and D. L. Lubin, "Compensated telescope system with programmable diffractive optic", Opt. Eng., 44 (2), 2005.